December 16, 2003
Preprint typeset using LaTeX style emulateapj

arXiv:astro-ph/0312348 v1 14 Dec 2003

ISOLATING GEOMETRY IN WEAK LENSING MEASUREMENTS

Jun Zhang[1,2], Lam Hui[1,2,3] and Albert Stebbins[1,3]
[1] Theoretical Astrophysics, Fermi National Accelerator Laboratory, Batavia, IL 60510
[2] Department of Physics, Columbia University, New York, NY 10027
[3] Department of Astronomy and Astrophysics, University of Chicago, IL 60637
jz203@columbia.edu, lhui@fnal.gov, stebbins@fnal.gov

December 16, 2003

ABSTRACT

Given a foreground galaxy-density field or shear field, its cross-correlation with the shear field from a background population of source galaxies scales with the source redshift in a way that is specific to lensing. Such a source-scaling can be exploited to effectively measure geometrical distances as a function of redshift and thereby constrain dark energy properties, free of any assumptions about the galaxy-mass/mass power spectrum (its shape, amplitude or growth). Such a geometrical method can yield a $\sim 0.03 - 0.07 f_{\rm sky}^{-1/2}$ measurement on the dark energy abundance and equation of state, for a photometric redshift accuracy of $\Delta z \sim 0.01 - 0.05$ and a survey with median redshift of ~ 1. While these constraints are weaker than conventional weak lensing methods, they provide an important consistency check because the geometrical method carries less theoretical baggage: there is no need to assume any structure formation model (*e.g.* CDM). The geometrical method is at the most conservative end of a whole spectrum of methods which obtain smaller errorbars by making more restrictive assumptions – we discuss some examples. Our geometrical approach differs from previous investigations along similar lines in three respects. First, the source-scaling we propose to use is less demanding on the photometric redshift accuracy. Second, the scaling works for both galaxy-shear and shear-shear correlations. Third, we find that previous studies underestimate the statistical errors associated with similar geometrical methods, the origin of which is discussed.

Subject headings: cosmology: theory — gravitational lensing — large-scale structure of universe — galaxies: halos — galaxies: structure

1. INTRODUCTION

Weak gravitational lensing has emerged to become an important probe of cosmology (*e.g.* Wittman *et al.* 2000, van Waerbeke *et al.* 2000, Bacon *et al.* 2000, Kaiser, Wilson, & Luppino 2000, Maoli *et al.* 2001, Rhodes *et al.* 2001, Hoekstra, Yee, & Gladders 2002, Jarvis *et al.* 2003, Pen *et al.* 2003; see review by Bartelmann & Schneider 2001). Much of the current discussion on potential dark energy constraints from weak lensing has focused on the use of the shear/convergence power spectrum, or equivalent measures, as a function of source redshift (*e.g.* Hu 2002, Abazajian & Dodelson 2003, Benabed & van Waerbeke 2003 but see *e.g.* Hui 1999, van Waerbeke *et al.* 2001, Benabed & Bernardeau 2001, Huterer 2002, Munshi & Wang 2003, Refregier *et al.* 2003, Takada & Jain 2003 for dark energy constraints from skewness or bispectrum). In these types of investigations, information about dark energy (both its abundance and equation of state) is encoded in the combination of geometrical distances and fluctuation growth rate that determines the observed lensing power spectrum. In this paper, we would like to pose and answer the question: is it possible to separate out the information purely from geometry i.e. irrespective of details of the mass power spectrum and its growth ? Such an exercise is useful because a method to do so allows us to derive dark energy constraints without making assumptions about the underlying large scale structure model (*e.g.* Cold Dark Matter, Gaussian initial conditions, etc). Comparing lensing constraints obtained via such a geometrical method against lensing constraints that carry more theoretical baggage provides an important consistency check. Moreover, a geometrical method allows us to make use of lensing measurements on small scales, scales which are often ignored in conventional methods because of worries about the ability to predict the nonlinear power spectrum accurately.

Our discussion is divided as follows. In §2, we point out an interesting scaling of lensing signals (i.e. shear-shear and galaxy-shear power spectra) with the source distance. Such a scaling can be used to obtain essentially an estimate of angular diameter distance (or more precisely, combinations of angular diameter distances) as a function of source redshift, without making any assumptions about the mass/galaxy power spectrum. We contrast this scaling with a different interesting scaling investigated by Jain & Taylor (2003), especially in terms of the demand on photometric redshift accuracy. The scaling we focus on can be applied to both galaxy-shear and shear-shear data, whereas the scaling of Jain & Taylor applies only to galaxy-shear. To understand what kind of constraints one could obtain about dark energy from our geometrical method, we perform a Fisher matrix analysis in §3. The conclusions are summarized in Fig. 1 and 2. The geometrical method above is a very conservative one: it makes absolutely no assumptions about the underlying large scale structure and its evolution. In §4 we investigate a method at the other end of the spectrum: it assumes the shape of the mass/galaxy power spectrum is known. It differs from more conventional methods (such as lensing tomography of Hu 2002, Abazajian & Dodelson 2003) only in that the geometrical information and growth rate information are separated to provide a consistency check. In

practice, there is of course a whole continuum of methods to obtain dark energy constraints from lensing data, varying from the most conservative (like the geometrical method emphasized here) to ones that make strong large scale structure assumptions. We conclude in §5.

A word on the history of this project is in order. When we started, our initial focus was on shear-shear correlation. Since then, an elegant paper by Jain and Taylor (2003, JT03 hereafter) appeared which addressed similar issues, but using the galaxy-shear correlation (see also interesting developments in Bernstein & Jain 2003 [BJ03]). Therefore we decide to include both in our discussion here. While our results are in qualitative agreement, we find quantitative differences. In particular we find dark energy constraints that are weaker than JT03. As we will explain in detail later, it is not *a priori* obvious whose constraints should be stronger. This is because we focus on a source-scaling of lensing signals that is different from JT03. Our scaling is less demanding on the photometric redshift accuracy and can be applied to both galaxy-shear and shear-shear correlation data, but introduces more free parameters. *However*, even if we employ exactly the same scaling adopted by JT03, we find statistical errors that are larger than JT03, the origin of which is discussed in detail in Appendix A. Related issues are discussed by Song & Knox (2003) and Hu & Jain (2003).

A word on terminology. JT03 used the term cross-correlation tomography to describe their method. This term can also be used to refer to the technique of cross-correlating shear/galaxy-density fields from different redshifts in general (e.g. Takada & White 2003). What we would like to focus on, as in the case of JT03, is the use of the cross-correlation technique to extract cosmological constraints that are purely geometrical in origin. To avoid confusion, we will generally not use the term cross-correlation tomography. We will simply refer to our approach as a geometrical method. To distinguish the source-scaling we exploit from the one used by JT03, we refer to ours as the offset-linear scaling (as opposed to the linear scaling adopted by JT03). The difference between these two scalings will be explained in the next section.

In the bulk of this paper, the term shear is loosely used to refer to its scalar part (i.e. the convergence). For simplicity, most of our expressions focus on correlations involving the convergence, and they assume a flat universe. Expressions for the more directly observable components of shear and for a non-flat universe are given in Appendix B.

2. A USEFUL SCALING OF LENSING SIGNALS WITH SOURCE DISTANCE

Here we consider several redshift distributions of galaxies some of which are considered foreground distribution (labeled by f) and other considered background galaxies (labeled by b). The idea being that the background galaxies are behind the foreground galaxies. One measures the lensing shear field of the different background galaxy populations and correlates it with either the shear field or the surface number density fluctuations of the foreground galaxies. By determining how these correlations scale with the redshift distribution of the background galaxies we hope to learn about the cosmology in a way which is independent of assumptions about inhomogeneities in the universe and depends only on the overall geometry.

It will be important that the foreground galaxies are indeed in front of the background galaxies and hence that they do not overlap in redshift with the background galaxies. [1] One can measure precisely using spectroscopy or estimate approximately using multi-color photometry the redshift distribution of the different populations. With spectroscopic redshifts it is a simple matter to assure that the foreground distribution and the background distribution overlap very little while with photometric redshifts this requires more care. In §3 below we will show how a small contamination of background galaxies in front of foreground galaxies affects the results.

In this paper we find it more useful to express everything in terms of comoving distance from the observer, χ, rather than redshift z. Of course, observationally one measures z and can only infer exact values of χ once one *assumes* a cosmology, which then gives you the function $\chi(z)$. The idea is to find cosmological parameters that give distances which best match the observed lensing correlations. Of crucial importance will be the z-distributions of galaxy populations, $dN(z)/dz$, but below we will use the distance distribution

$$W(\chi(z)) \equiv \frac{\frac{dN(z)}{dz}}{\frac{d\chi(z)}{dz}\int_0^\infty dz' \, \frac{dN(z')}{dz'}} \tag{1}$$

so that $\int d\chi \, W(\chi) = 1$. We will add a f or b subscript to W for foreground or background populations, respectively. Other cosmological quantities we will use are the scale factor $a(\chi)$ defined by $a(\chi(z)) = 1/(1+z)$, the Hubble parameter $H(\chi) = -ca'(\chi)/a(\chi)^2$, and $\Omega_{\rm m0}$ is the present density of matter (dark + baryonic) in units of the critical density. We define $H_0 \equiv H(0)$ and c is the speed of light.

For simplicity we assume a flat universe in the bulk of the paper. All expressions, in particular the scaling of interest, can be generalized to a non-flat universe as discussed in Appendix B. Also, the expressions in the bulk of the paper are given in Fourier space. The real space counterparts are discussed in Appendix B as well.

We are interested in 2 kinds of correlations. One is correlating the background shear (γ) field with the foreground galaxy density field, and the other is with some foreground γ field. The first is usually referred to as *galaxy-galaxy lensing* and the second is known as *shear-shear correlation.* In both cases the shear that is correlated is only the scalar (a.k.a. G-mode or E-mode) component of the shear pattern [2] (see Stebbins 1996). Unless otherwise stated, we will use γ to refer to this scalar part: the convergence. Using a Limber approximation for small angles (large ℓ) the resulting angular cross power spectra, $P_{\rm g\gamma}(\ell)$ and $P_{\gamma\gamma}(\ell)$ can be written as (Blandford et al. 1991, Miralda-Escude 1991, Kaiser 1992, Jain & Seljak 1997)

$$P_{\rm g\gamma}(\ell; f, b) = \frac{3\Omega_{\rm m0}H_0^2}{2c^2}\int \frac{d\chi_{\rm f}}{a(\chi_{\rm f})} W_f(\chi_{\rm f}) \int d\chi_{\rm b} W_b(\chi_{\rm b})$$

[1] However, it is completely unimportant whether different background (or foreground) populations overlap, or even whether they contain common members.

[2] Also known as "electric-", or "gradient-" component. This excludes the other component, known as "curl-", "C-", "magnetic-", "B-', or pseudoscalar- component, which will have a much smaller signal and less useful information for our purposes.

$$\times \frac{\chi_{\rm b}-\chi_{\rm f}}{\chi_{\rm b}\chi_{\rm f}}\, P_{{\rm g}\delta}(\frac{\ell}{\chi_{\rm f}},\chi_{\rm f})\,\Theta(\chi_{\rm b}-\chi_{\rm f}) \quad (2)$$

and

$$P_{\gamma\gamma}(\ell;f;b) = \left(\frac{3\Omega_{\rm m0}H_0^2}{2c^2}\right)^2 \quad (3)$$
$$\times \int d\chi_{\rm f} W_f(\chi_{\rm f}) \int d\chi_{\rm b} W_b(\chi_{\rm b})$$
$$\times \int \frac{d\chi}{a(\chi)^2}\frac{\chi_{\rm b}-\chi}{\chi_{\rm b}}\frac{\chi_{\rm f}-\chi}{\chi_{\rm f}} P_{\delta\delta}(\frac{\ell}{\chi},\chi)\Theta(\chi_{\rm b}-\chi)\,\Theta(\chi_{\rm f}-\chi).$$

Here $\Theta(\chi_{\rm b}-\chi)$ is the Lorentz-Heaviside function which is unity if $\chi < \chi_{\rm b}$, and zero otherwise. Also $P_{g\delta}(k,\chi)$ and $P_{\delta\delta}(k,\chi)$ are respectively the 3-d galaxy-mass power spectrum and 3-d mass power spectrum, both evaluated at 3-d wavenumber k and at a time corresponding to distance χ, and ℓ is the angular wavenumber. As always with the Limber approximation there is a one-to-one correspondence with the 3-d wavenumber and angular wavenumber at a given distance χ: $k \leftrightarrow \frac{\ell}{\chi}$.

2.1. *Offset-Linear Scaling*

The key step for the purpose of this paper is to note that if the foreground distribution W_f and the background distribution W_b overlap very little then it is an excellent approximation to make the substitution

$$W_f(\chi_{\rm f})\,W_b(\chi_{\rm b})\,\Theta(\chi_{\rm b}-\chi_{\rm f}) \rightarrow W_f(\chi_{\rm f})\,W_b(\chi_{\rm b}) \quad (4)$$

in eq. [2], or

$$W_f(\chi_{\rm f})\,W_b(\chi_{\rm b})\,\Theta(\chi_{\rm b}-\chi)\,\Theta(\chi_{\rm f}-\chi) \quad (5)$$
$$\rightarrow W_f(\chi_{\rm f})\,W_b(\chi_{\rm b})\,\Theta(\chi_{\rm f}-\chi).$$

in eq.[3]. Under this approximation the angular power spectrum will exhibit an *offset-linear scaling*:

$$P_{{\rm g}\gamma}(\ell;f,b) \approx F(\ell;f) + G(\ell;f)/\chi_{\rm eff}(b) \quad (6)$$
$$P_{\gamma\gamma}(\ell;f,b) \approx A(\ell;f) + B(\ell;f)/\chi_{\rm eff}(b)$$

where

$$\frac{1}{\chi_{\rm eff}(b)} \equiv \int d\chi_{\rm b} W_b(\chi_{\rm b})\,\frac{1}{\chi_{\rm b}} \quad (7)$$

and

$$F(\ell;f) \equiv \frac{3\Omega_{\rm m0}H_0^2}{2c^2}\int \frac{d\chi_{\rm f}}{a(\chi_{\rm f})}\frac{W_f(\chi_{\rm f})}{\chi_{\rm f}} P_{g\delta}(\frac{\ell}{\chi_{\rm f}},\chi_{\rm f}) \quad (8)$$
$$G(\ell;f) \equiv -\frac{3\Omega_{\rm m0}H_0^2}{2c^2}\int \frac{d\chi_{\rm f}}{a(\chi_{\rm f})}\,W_f(\chi_{\rm f})\,P_{g\delta}(\frac{\ell}{\chi_{\rm f}},\chi_{\rm f})$$
$$A(\ell;f) \equiv \left(\frac{3\Omega_{\rm m0}H_0^2}{2c^2}\right)^2 \int d\chi_{\rm f}\,W_f(\chi_{\rm f})$$
$$\times \int_0^{\chi_{\rm f}} \frac{d\chi}{a(\chi)^2}\,\frac{\chi_{\rm f}-\chi}{\chi_{\rm f}}\,P_{\delta\delta}(\frac{\ell}{\chi},\chi)$$
$$B(\ell;f) \equiv -\left(\frac{3\Omega_{\rm m0}H_0^2}{2c^2}\right)^2 \int d\chi_{\rm f}\,W_f(\chi_{\rm f})$$
$$\times \int_0^{\chi_{\rm f}} \frac{d\chi}{a(\chi)^2}\,\frac{\chi_{\rm f}-\chi}{\chi_{\rm f}}\,\chi\,P_{\delta\delta}(\frac{\ell}{\chi},\chi)$$

This is the scaling we wish to exploit: for a fixed foreground population, W_f, as one varies the background redshift distribution W_b, the lensing power spectra $P_{{\rm g}\gamma}$ and $P_{\gamma\gamma}$ scale in a definite manner, namely linearly through the factor $1/\chi_{\rm eff}(b)$ but with an offset given by F or A (hence the name *offset-linear scaling*). This should be contrasted with the linear scaling described below. Moreover, this factor $1/\chi_{\rm eff}(b)$ is purely geometrical. It is the inverse source distance averaged over the background redshift distribution (eq. [7]). It is important to emphasize that eq. [6] holds even if W_f and W_b are broad distributions – the only requirement is that they have little overlap. We will discuss what requirement this places on the photometric redshift accuracy in §3.

Such a scaling is very useful in confirming the lensing hypothesis of the observed correlation *i.e.* intrinsic alignment is not expected to produce this kind of scaling. This fact can be exploited to weed out contamination of the observed signals from intrinsic alignment, which will be further explored in a future paper.

A more ambitious goal is to use this scaling to effectively measure the angular diameter distance as a function of redshift (more precisely, measure $\chi_{\rm eff}(b)$ as a function of distribution W_b), and use this to constrain cosmological parameters, especially those pertaining to dark energy, in a way independent of assumptions about the large scale structure of galaxy and mass. This is the topic of §3.

2.2. *Comparison with Linear Scaling*

At this point, it is useful to compare the scaling displayed in eq. [6] with the scaling used by JT03. Unlike offset-linear scaling, the JT03 scaling can only be applied to $P_{{\rm g}\gamma}$, *i.e.* to galaxy-galaxy lensing. JT03 assumed W_f is well approximated by a delta function at a distance, $\hat{\chi}_{\rm f}$, in which case $G(\ell;f) = -\hat{\chi}_{\rm f}\,F(\ell;f)$ and $P_{{\rm g}\gamma}$ follows a scaling that is even simpler than in eq. [6] (although eq. [6] still holds) *i.e. a linear scaling* with no offset:

$$P_{{\rm g}\gamma}(\ell;f,b) \approx F(\ell;f)\,\left(1-\frac{\hat{\chi}_{\rm f}}{\chi_{\rm eff}(b)}\right) \quad (9)$$

Note that all of the uncertainties associated with large scale structure come in the prefactor $F(\ell;f)$. Here the background distribution, W_b, does not have to be well approximated by a δ-function, only the foreground distribution, W_f, does. One also requires that W_b not extend significantly into the foreground just as with the offset-linear scaling. For a fixed foreground redshift, varying the background distribution produces a definite *linear scaling* (with no offset) of $P_{{\rm g}\gamma}$ with the geometrical factor $1-\hat{\chi}_{\rm f}/\chi_{\rm eff}(b)$. JT03 proposed that one can examine the ratio of $P_{{\rm g}\gamma}$'s measured using two different background distributions (W_b and $W_{b'}$) but the same foreground: [3]

$$\frac{P_{{\rm g}\gamma}(\ell;f,b)}{P_{{\rm g}\gamma}(\ell;f,b')} \approx \frac{\hat{\chi}_{\rm f}^{-1}-\chi_{\rm eff}(b)^{-1}}{\hat{\chi}_{\rm f}^{-1}-\chi_{\rm eff}(b')^{-1}}. \quad (10)$$

One can infer values for cosmological parameters with this equation by measuring the left-hand-side and then finding the parameters for which the right-hand-side yield the same values.

[3] We have paraphrased JT03 a little bit here. They considered the ratio of correlations measured in real space instead of Fourier space.

2.3. *The Foreground Width Systematic*

In practice the foreground galaxies will not have zero uncertainty in distance, and unless one has spectroscopic redshifts for the foreground galaxies (*e.g.* McKay et al. 2001, Sheldon et al. 2003), W_f will have some non-negligible spread. Such a spread implies the ratio of the observed $P_{\rm g\gamma}$'s will differ from the idealized limit of eq. [10] which can lead to systematic errors in estimates of cosmological parameters, *e.g.* the dark energy equation of state, w, if one uses the linear scaling but not if one uses the offset-linear scaling.

If the foreground distribution W_f is not a delta function, eq.s [9,10] should be replaced by:

$$P_{\rm g\gamma}(\ell; f, b) \approx F(\ell; f)\left(1 - \frac{\tilde{\chi}_{\rm f}}{\chi_{\rm eff}(b)}\right) \tag{11}$$

$$\frac{P_{\rm g\gamma}(\ell; f, b)}{P_{\rm g\gamma}(\ell; f, b')} \approx \frac{\tilde{\chi}_f(\ell)^{-1} - \chi_{\rm eff}(b)^{-1}}{\tilde{\chi}_f(\ell)^{-1} - \chi_{\rm eff}(b')^{-1}} \tag{12}$$

where $\tilde{\chi}_f(\ell) \equiv -G(\ell; f)/F(\ell; f)$. While eq.s [10,12] are similar in form the right-hand-side of the latter is ℓ dependent and depends on non-measured and non-geometrical quantities like the galaxy-mass power spectrum $P_{\rm g\delta}(k, \chi)$.

To bring the non-geometrical character of eq. [12] into better focus, let us perform an expansion of $\tilde{\chi}_f$ around the mean distance $\bar{\chi}_f \equiv \int d\chi_{\rm f} W_f(\chi_{\rm f})\, \chi_{\rm f}$ *i.e.* $\tilde{\chi}_f = \bar{\chi}_f + \Delta\chi_{f(2)} + \Delta\chi_{f(3)} + \ldots$ where $\Delta\chi_{f(n)}$ is order n in the width of W_f (the 1st order term is zero). The lowest order correction is

$$\Delta\chi_{f(2)}(\ell) = -\frac{\sigma_\chi^2}{\bar{\chi}_f} \times \left(1 - \frac{a_f\, \bar{\chi}_f\, H_f}{c} + n_f(\ell) + \frac{2\, a_f H_f \bar{\chi}_f\, \Upsilon_f(\ell)}{c}\right) \tag{13}$$

where σ_χ is the width of W_f *i.e.* $\sigma_\chi^2 \equiv \int d\chi_{\rm f} W_f(\chi_{\rm f})(\chi_{\rm f} - \bar{\chi}_f)^2$, $a_f \equiv a(\bar{\chi}_f)$, $H_f \equiv H(\bar{\chi}_f)$ is the Hubble constant at the time corresponding to $\bar{\chi}_f$,

$$n_f(\ell) \equiv \left.\frac{d{\rm ln}P_{\rm g\delta}(k, \bar{\chi}_f)}{d{\rm ln}k}\right|_{k=\frac{\ell}{\bar{\chi}_f}} \tag{14}$$

is the spectral index evaluated at that foreground redshift, and

$$\Upsilon_f(\ell) \equiv \frac{1}{2}\left.\frac{d{\rm ln}P_{\rm g\delta}(\frac{\ell}{\bar{\chi}_f}, \chi)}{d{\rm ln}a(\chi)}\right|_{\chi=\bar{\chi}_f} \tag{15}$$

tells us about the growth of correlations with time.

The terms $n_f(\ell)$ and $\Upsilon_f(\ell)$ in $\Delta\chi_{f(2)}(\ell)$ clearly depend on a non-geometrical quantity, namely the 3-d galaxy-mass power spectrum $P_{g\delta}(k, \bar{\chi}_f)$. One can imagine improving upon the JT03 procedure by accounting for corrections due to such terms when fitting the ratio of lensing correlations for dark energy parameters (eq. [12]). This somewhat compromises the original goal of isolating the purely geometrical information. A more serious problem is that a quantity like $\Upsilon_f(\ell)$, which is the growth rate of the galaxy-mass correlation, is fundamentally rather uncertain because of the uncertain relation between galaxy and mass. Conservatively, this leads to an order $\sigma_\chi^2/\bar{\chi}_f$ uncertainty in any estimate of the correction $\Delta\chi_{f(2)}(\ell)$.

In other words, as long as the foreground distribution W_f has a finite width, the ratio of correlations considered by JT03 does not give eq. (10), but instead gives eq. (12), where $\tilde{\chi}_f = \bar{\chi}_f + O(\sigma_\chi^2/\chi_f)$ and the correction $O(\sigma_\chi^2/\chi_f)$ is uncertain. Attempts to make use of the JT03 linear scaling to infer dark energy constraints is therefore subject to a systematic error that depends on the width of W_f. Following JT03, consider using a foreground distribution by taking a photometric redshift bin centered at for instance $z_p = 0.3$, with a top-hat width of $\Delta z_p = 0.1$. To obtain the actual distribution W_f of *true* redshifts, one has to convolve such a top-hat photometric redshift bin with the photometric redshift error distribution, which we model as a Gaussian of dispersion σ_z (this is described more fully in §3). We find that the JT03 method (eq. [12]) is susceptible to a systematic error of $\sim$ 30%, 5% or 1% on the dark energy equation of state w, for $\sigma_z = 0.05$, 0.02 or 0.01 respectively. The JT03 linear scaling is therefore quite demanding on the photometric redshift accuracy if one would like to keep the systematic error below say 1%. Unless spectroscopic redshifts are available, we think it is more productive to make use of the offset-linear scaling which makes no assumptions about the width of W_f and can be applied to both pure lensing data and galaxy-galaxy lensing.

2.4. *The Ratio of Power Spectrum Differences*

For a zero width foreground galaxy distribution linear scaling means the ratio of the power spectrum leads to a purely geometric expression (eq. [10]), while more generally with offset-linear scaling it is the ratio of difference of power spectra which is purely geometrical:

$$\frac{P(\ell; f, b) - P(\ell; f, b')}{P(\ell; f, b'') - P(\ell; f, b''')} = \frac{\chi_{\rm eff}(b)^{-1} - \chi_{\rm eff}(b')^{-1}}{\chi_{\rm eff}(b'')^{-1} - \chi_{\rm eff}(b''')^{-1}} \tag{16}$$

where here P can be either $P_{\gamma\gamma}$ or $P_{\rm g\gamma}$. Here we illustrate the general case of 4 background populations b, b', b'', b'''; but the expression still gives a non-trivial result for 3 populations, say if $b = b''$. Unlike eq. [10] this expression makes no assumptions about the width of W_f being small. It does not depend on the mass power spectrum or its growth, but depends only on the background redshift distributions and cosmological parameters of interest, such as the equation of state and abundance of dark energy.

2.5. *The Redshift Tail Systematic*

Another systematic effect which is common to *both* linear and offset-linear scaling comes from the approximations of eq.s [4,5] that the foreground populations are completely in front of the background populations. If this is not true then the eq. [6] is not exact, but the exact expression is

$$\begin{aligned} P_{\rm g\gamma}(\ell; f, b) &= F(\ell; f) + G(\ell; f)/\chi_{\rm eff}(b) + I(\ell; f, b) \\ P_{\gamma\gamma}(\ell; f, b) &= A(\ell; f) + B(\ell; f)/\chi_{\rm eff}(b) + D(\ell; f, b) \end{aligned} \tag{17}$$

where the additional terms are given by

$$I(\ell; f, b) \equiv \frac{3\Omega_{\rm m0} H_0^2}{2c^2}\int_0^\infty \frac{d\chi_{\rm f}}{a(\chi_{\rm f})} W_f(\chi_{\rm f}) \tag{18}$$

$$\times \int_0^{\chi_{\rm f}} d\chi_{\rm b} W_b(\chi_{\rm b}) \, \frac{\chi_{\rm f}-\chi_{\rm b}}{\chi_{\rm b}\chi_{\rm f}} \, P_{g\delta}(\frac{\ell}{\chi_{\rm f}}, \chi_{\rm f})$$

$$D(\ell; f, b) \equiv \left(\frac{3\Omega_{\rm m0} H_0^2}{2c^2}\right)^2 \int_0^{\infty} d\chi_{\rm f} \, W_f(\chi_{\rm f})$$

$$\times \int_0^{\chi_{\rm f}} d\chi_{\rm b} \, W_b(\chi_{\rm b}) \int_{\chi_{\rm b}}^{\chi_{\rm f}} \frac{d\chi}{a(\chi)^2} \, \frac{\chi-\chi_{\rm b}}{\chi_{\rm b}} \, \frac{\chi_{\rm f}-\chi}{\chi_{\rm f}} \, P_{\delta\delta}(\frac{\ell}{\chi}, \chi) \ ,$$

which are both positive (at least so long as $P_{g\delta} > 0$). The ratio of power spectrum differences is given by eq. [16] only to the extent that the additional terms I or D are negligible. Note that I and D are non-zero only when the foreground distribution $W_f(\chi_f)$ and background distribution $W_b(\chi_b)$ have non-vanishing overlap *i.e.* some of the galaxies identified as foreground are actually behind the galaxies identified as background ($\chi_f > \chi_b$). This systematic effect differs from the foreground width systematic discussed earlier in that it depends on the tail of the distributions of redshift uncertainties. This is different from a systematic caused by the width of the foreground distribution because one can reduce the overlap, and hence the systematic, by selecting the foreground and background populations in a way which further separates them in redshift. Since the tail of the redshift distribution is likely to fall off rapidly, increasing the separation can greatly decrease the amount of overlap, and hence the size of I and D, and therefore inaccuracy of eq. [16]. In contrast the foreground width systematic, which only effect the linear scaling, is not decreased by further separating the foreground and background populations. We quantify how large a systematic error this effect will have on our analysis in §3.

3. A FISHER MATRIX ANALYSIS EXPLOITING THE SOURCE SCALING

Here, we would like to find out the dark energy constraints one can in principle obtain from the offset-linear scaling described in eq. [6], using purely geometric quantities like eq. [16]. Given several redshift bins, one can imagine there are many ways, or at least many combinations like eq. [16], to obtain dark energy constraints. Given a set of $P_{\rm g\gamma}(\ell; f, b)$'s and $P_{\gamma\gamma}(\ell; f, b)$'s for a whole range of f, b, the best way is probably to fit them using the offset-linear scaling of eq. [6], and marginalize over A,B,F and G.

To estimate the statistical errors, we will assume the mass and galaxy density fields are approximated by Gaussian random noise. On large scales, the near Gaussianity of cosmological inhomogeneities is quite well established. Even on small scales where the 3-d mass and galaxy distribution are far from Gaussian, the projected galaxy and mass surface density (which gives the shear) are much more Gaussian since they are a projection of many 3-d structures (Scoccimarro, Zaldarriaga, & Hui 1999, White & Hu 2000, Cooray & Hu 2001). The expected non-Gaussianity will lead to a small underestimate of errorbars but does not lead to a bias.

To predict the uncertainties in cosmological parameters we use a Fisher matrix calculation. For a zero mean Gaussian distribution the Fisher matrix element for parameters p_α and p_β is given by (*e.g.* Tegmark 1997)

$$F_{\alpha\beta} = \frac{1}{2} \, {\rm Tr} \left[\mathbf{C}^{-1} \cdot \frac{\partial \mathbf{C}}{\partial p_\alpha} \cdot \mathbf{C}^{-1} \cdot \frac{\partial \mathbf{C}}{\partial p_\beta} \right] \tag{19}$$

where $\mathbf{C}$ is the correlation matrix of the data vector $\mathbf{d}$, *i.e.* $\mathbf{C} \equiv \langle \mathbf{d}^{\rm T} \mathbf{d} \rangle$. [4] Here the elements of $\mathbf{d}$ might consist of local (in angle) shear and galaxy surface density estimators, however it is more convenient to make linear combinations which, for each distance bin (foreground or background), are mode amplitudes for approximate eigenmodes of the angular Laplace operator, with approximate eigenvalue $-\ell\,(\ell+1)$ (for shear we want only the scalar (E-) eigenmodes). Discrete sampling by galaxies and incomplete sky coverage will prevent one from constructing exact eigenmodes in practice, but to estimate the errors it is a good approximation[5] to assume that such modes exist, that the different angular modes are uncorrelated, and the number of modes with wavenumber ℓ is $(2\ell+1)\, f_{\rm sky}$ where $f_{\rm sky}$ is the fraction of the sky one has surveyed. Since the modes are uncorrelated and the modes for the same angular wavenumber, ℓ, should have the same correlations, the correlation matrix $\mathbf{C}$ is block diagonal, and we may rewrite the Fisher matrix element as

$$F_{\alpha\beta} = f_{\rm sky} \sum_\ell (2\ell+1) \, F_{\ell,\alpha\beta} \tag{20}$$

where

$$F_{\ell,\alpha\beta} = \frac{1}{2} {\rm Tr} \left[\mathbf{C}_\ell^{-1} \cdot \frac{\partial \mathbf{C}_\ell}{\partial p_\alpha} \cdot \mathbf{C}_\ell^{-1} \cdot \frac{\partial \mathbf{C}_\ell}{\partial p_\beta} \right] \ . \tag{21}$$

If there are $n_{\rm bin}$ redshift bins each $\mathbf{C}_\ell$ block can be divided into $n_{\rm bin} \times n_{\rm bin}$ sub-blocks as follows

$$\mathbf{C}_\ell \equiv \begin{pmatrix} \mathbf{C}_{\ell,1,1} & \cdots & \mathbf{C}_{\ell,1,n_{\rm bin}} \\ \vdots & \ddots & \vdots \\ \mathbf{C}_{\ell,n_{\rm bin},1} & \cdots & \mathbf{C}_{\ell,n_{\rm bin},n_{\rm bin}} \end{pmatrix} \ , \tag{22}$$

one for each ordered pair of distance bins, (i, j). The sub-blocks are 2×2 matrices given by

$$\mathbf{C}_{\ell,i,j} \equiv \begin{pmatrix} P_{\rm gg}(\ell; i, j) + \delta_{ij} \frac{1}{\bar{n}_i^g} & P_{\rm g\gamma}(\ell; i, j) \\ P_{\rm g\gamma}(\ell; j, i) & P_{\gamma\gamma}(\ell; i, j) + \delta_{ij} \frac{\sigma^2_{\gamma,i}}{\bar{n}_i^{\rm g}} \end{pmatrix} \tag{23}$$

where $P_{gg}(\ell; i, j)$ is the cross power spectrum at wavenumber ℓ of galaxies in redshift bin i and bin j, $\bar{n}_i^{\rm g}$ is the surface density of galaxies in redshift bin i which tells us the *shot noise*, and $\sigma^2_{\gamma,i}$ is the intrinsic noise of the shear from one galaxy in redshift bin i which tells us the *shape noise*. Since $P_{\rm gg}(\ell; i, j) = P_{\rm gg}(\ell; j, i)$ and $P_{\gamma\gamma}(\ell; i, j) = P_{\gamma\gamma}(\ell; i, j)$ we see that $\mathbf{C}_{\ell,i,j} = \mathbf{C}^{\rm T}_{\ell,j,i}$ and that $\mathbf{C}_\ell$ is symmetric. If the redshift bins are reasonably large, it will be a good

[4] BJ03 also performed a Fisher matrix analysis. Their starting point was different from ours, however (in addition to other differences discussed in Appendix A). BJ03 started from a likelihood that treated the power spectra themselves as data which are Gaussian distributed.

[5] This is true when most of the Fisher information comes from angular scales much smaller than the survey size and much greater than the typical inter-galaxy separation.

approximation to ignore galaxy correlations between bins, *i.e.* we assume $P_{\rm gg}(\ell;i,j)=\delta_{ij}P_{\rm gg}(\ell;i)$.

We suppose that the galaxies in each population have measured *photometric* redshifts, $z_{\rm p}$ which estimate the true redshift. We assume that the distribution of $z_{\rm p}$ from all galaxies in all bins is

$$\frac{dN_{\rm p}(z_{\rm p})}{dz_{\rm p}} \propto z_{\rm p}^2\, e^{-\left(\frac{z_{\rm p}}{1.0}\right)^{1.5}} \quad . \tag{24}$$

We divide this total population into $n_{\rm bin}$ top-hat bins in $z_{\rm p}$-space, such that bin i contains all galaxies with $(i-1)\,\Delta z_{\rm p} \le z_{\rm p} < i\,\Delta z_{\rm p}$. We suppose the photometric redshifts are unbiased estimators of the true redshift with errors distributed like a Gaussian with variance σ_z^2 so that the distribution of true redshifts in bin i is

$$\frac{dN_i(z)}{dz} \propto \int_{(i-1)\,\Delta z_{\rm p}}^{i\,\Delta z_{\rm p}} dz_{\rm p}\, \frac{dN_{\rm p}(z_{\rm p})}{dz_{\rm p}}\, e^{-\frac{1}{2}\left(\frac{z-z_{\rm p}}{\sigma_z}\right)^2} \tag{25}$$

which then is related to $W_i(\chi)$ through eq. [1] and from that we can compute, for a given set of cosmological parameters, the effective distance to each bin, $\chi_{\rm eff}(i)$, from eq [7].

Note that we have not yet defined foreground and background bins or exploited offset-linear scaling. To do so we define foreground/background pairs by the requirement that bin j is a background bin to bin i if $j \ge i+\Delta_{\rm bin}$. If $b=j$ is a background bin to foreground bin $f=i$ then $P_{\rm g\gamma}(\ell;f,b)$ and $P_{\gamma\gamma}(\ell;f,b)$ are given by eq. 6 while $P_{\rm g\gamma}(\ell;b,f)=0$ and $P_{\gamma\gamma}(\ell;b,f)=P_{\gamma\gamma}(\ell;f,b)$. One minimally requires that $\Delta_{\rm bin}=1$, however in this case one is subject to systematics by the redshift tail to the extent that the redshift distributions between adjacent bins overlap. Increasing $\Delta_{\rm bin}$ decreases any systematic effect from redshift tails, however it also leads to larger statistical errors because more information is thrown away. We will discuss below the choice of $\Delta_{\rm bin}$ and redshift binning.

The correlation matrix depends on several functions having to do with the power spectrum: there are the foreground functions $A(\ell;f)$, $B(\ell;f)$, $F(\ell,f)$, and $G(\ell,f)$; and then there are the lensing power spectra $P_{\rm g\gamma}(\ell;i,j)$ and $P_{\gamma\gamma}(\ell;i,j)$ where neither $\{i,j\}$ nor $\{j,i\}$ forms a foreground-background pair (as defined above via $\Delta_{\rm bin}$); finally there are the galaxy angular power spectra $P_{gg}(\ell;i,j)$. These are functions we are not interested in because we are only interested in obtaining constraints on dark energy properties which are independent of the values of these functions. So we assume their values are not known *a priori*, and for each ℓ we take their values to be unknown *nuisance parameter*s, *i.e.* each corresponding to one component of p_α. So the number of unknown parameters will be very large, but since dependence on each of these uninteresting parameters is confined to a single block, $\mathbf{C}_\ell$, the computation of the Fisher matrix remains tractable.

In addition to the nuisance parameters the correlation matrix depends on the background bin distances: $\chi_{\rm eff}(b)$ (eq. [7]). These will depend on interesting cosmological parameters through the function $\chi(z)$ and eq. [1]. The cosmological parameters we are actually interested in are: w the equation of state of dark energy, $w'\equiv dw/dz$, and $\Omega_{\rm de}$ the dark energy density today in unit of the critical density. We assume a flat universe here, so the matter density is given by $\Omega_{\rm m0}=1-\Omega_{\rm de}$.

To remove the nuisance parameters we can marginalize over their values. This can be done by inverting the full Fisher matrix, $F_{\alpha\beta}$, and then restricting the inverse to the interesting cosmological parameters, let us denote them by $\tilde\alpha,\tilde\beta$:[6]

$$\widetilde{E}_{\tilde\alpha\tilde\beta} \equiv (F^{-1})_{\tilde\alpha\tilde\beta} \tag{26}$$

According to the Cramer-Rao inequality the minimum possible error ellipses in parameter space (for unbiased estimators) have principal axes in the directions of the eigenvectors of $\widetilde{E}_{\tilde\alpha\tilde\beta}$ with size given by the square root of the corresponding eigenvalues of $\widetilde{E}_{\tilde\alpha\tilde\beta}$. Maximum likelihood parameter estimators (MLEs) will approach this accuracy where the errorbars are small enough. For the problem at hand we expect these minimum errors to close to what can be obtained in practice.

To obtain prediction for how accurately one can constrain cosmological parameters using offset-linear scaling, we take $f_{\rm sky}=0.1$, (*i.e.* a $4000\,(^\circ)^2$ survey), $\sigma^2_{\gamma,i}=0.3^2/2$ (shape noise), and $\sum_{i=1}^{n_{\rm bin}}\bar n_i^{\rm g}=100/(')^2$. For the fiducial cosmological and structure formation model, we use $w=-1$, $\Omega_{\rm de}=0.7$, a scale invariant primordial mass power spectrum with a linear amplitude of $\sigma_8=0.9$, and for the galaxy and galaxy-mass power spectra, we employ the halo model (Sheth & Jain 1997, Ma & Fry 2000, Seljak 2000, Scoccimarro et al. , Guzik and Seljak 2001). To distribute galaxies inside halos, we use the occupation function given by Kratsov et al. (2003), with a galaxy (subhalo) masscut at each redshift that matches the redshift distribution given in eq. [24] with a total integrated number density of $\sum_{i=1}^{n_{\rm bin}}\bar n_i^{\rm g}=100/(')^2$. We have experimented with using only the more massive halos as foreground following JT03, but found it did not lead to an improvement in statistical errors.

Carrying out the Fisher matrix calculation as outlined above we obtain the dark energy constraints as shown in Fig. 1 and Fig. 2 which show, respectively the constraints on $\Omega_{\rm de}$ and w when $w'=0$, and the constraints on w and w' when $\Omega_{\rm de}$ is assumed to be known to 3%. The symbol w' denotes dw/dz. A common alternative parametrization of evolution of w has $w_a=2w'$ at $z=1$ (Linder 2002). The solid, dashed and dotted contours give 1 σ errors that correspond to a photometric redshift accuracy of $\sigma_z=0.01, 0.02$ and 0.05 respectively. For each photometric redshift accuracy, we choose a redshift binning that keeps the redshift tail systematic error (§2.5) at a sub-percent level while minimizing the statistical error. (Keeping the systematic error on dark energy parameters at a sub-percent level is probably more stringent than is necessary given the size of the statistical error as it turns out.) For a photometric redshift error of $\sigma_z=0.05$, we choose $(\Delta z_{\rm p}, n_{\rm bin}, \Delta_{\rm bin})=(0.15,20,2)$; for $\sigma_z=0.02$, we choose $(0.1,30,2)$, and for $\sigma_z=0.01$, we consider $(0.15,20,1)$. The values of σ_z considered should span a reasonable range of what can be achieved with photometric redshifts. The redshift bins stretch out to $z\sim 3$ which encompasses the redshift range of most normal galaxies. Sampling photo-

[6] In order for $F_{\alpha\beta}$ to be invertible we require that $n_{\rm bin}\ge\Delta_{\rm bin}+3$ otherwise there are never the 3 background bins required to construct the ratio of power spectrum differences, eq. [16], so that one can make use of the offset-linear scaling.

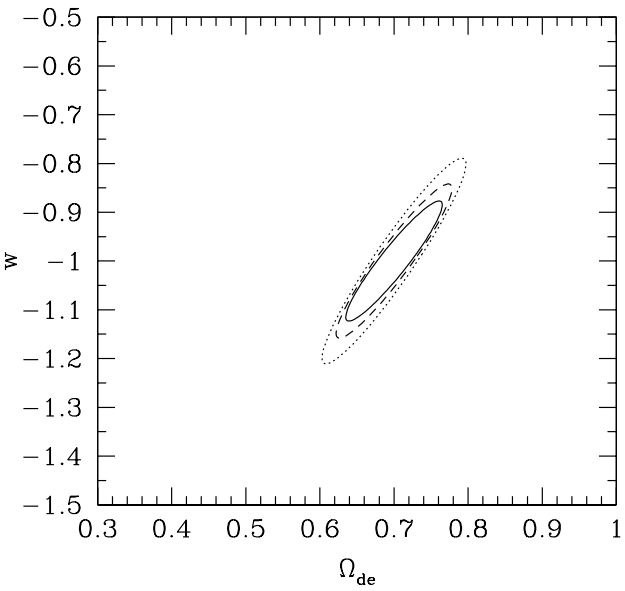

FIG. 1.— Purely geometrical weak-lensing constraints on w and $\Omega_{\rm de}$, making use of the offset-linear scaling of eq. [6], for a survey covering 10% of the sky, and median redshift ~ 1 (eq. [24]). The solid, dashed and dotted (1 σ) contours correspond to a photometric redshift error of $\sigma_z = 0.01, 0.02$ and 0.05 respectively. The size of σ_z is relevant only because the redshift bins are chosen to keep systematic error below 1%, and the statistical error is affected by the redshift binning (see text). The equation of state w is assumed constant. No prior is placed on $\Omega_{\rm de}$ or w. The fiducial model has $w = -1$ and $\Omega_{\rm de} = 0.7$.

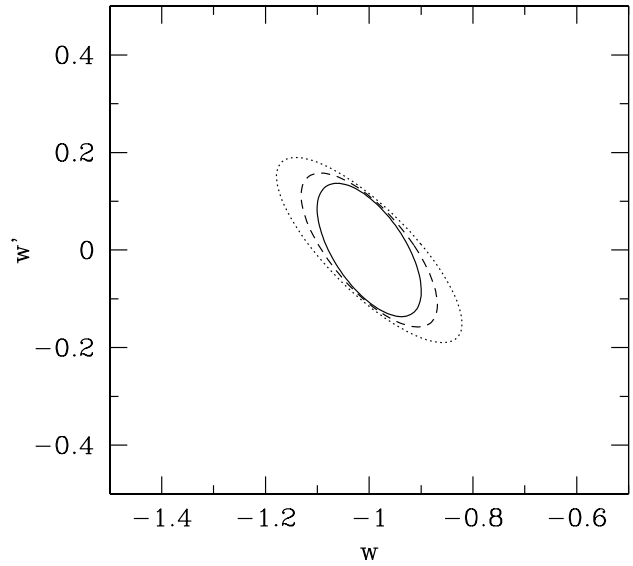

FIG. 2.— Purely geometrical weak-lensing constraints on w and w', making use of the offset-linear scaling of eq. [6], for a survey covering 10% of the sky, and median redshift ~ 1 (eq. [24]). The solid, dashed and dotted contours have the same meanings as in Fig. 1. A 3% uncertainty on $\Omega_{\rm de}$ is assumed. The fiducial model has $w = -1$, $w' = 0$ and $\Omega_{\rm de} = 0.7$, where $w' \equiv dw/dz$. Note that a common alternative parametrization has $w_a = 2w'$ at $z = 1$ (see text).

metric redshift space more finely by decreasing $\Delta z_{\rm p}$ while increasing $n_{\rm bin}$ accordingly gives negligible improvement in errorbars mainly because of the increased importance of shot-noise when the bin size is made small (see Hu 1999).

Note that because we marginalize over all parameters that are determined by the mass, galaxy and galaxy-mass power spectra, it is sensible for us to use information from all scales (from the fundamental mode to $\ell \sim 10^5$)– *i.e.* there is no need to stay away from nonlinear scales because of worries about how well one can predict the mass and galaxy power spectra. Of course, at sufficiently high ℓ's, shape-noise dominates and not much information is gained from the very high ℓ modes.

Fig.s 1 & 2 show that our geometrical method employing offset-linear scaling yields weaker dark energy constraints than conventional weak lensing methods which make more assumptions about the structure formation model (w generally constrained at the few percent level for a comparable survey as above; see *e.g.* Hu 2002, Abazajian & Dodelson 2003). This is of course not surprising, since the offset-linear scaling method throws away non-geometrical information that is utilized in conventional methods. However, the geometrical constraints are still sufficiently tight to provide an interesting consistency check: dark energy constraints obtained using the two different methods should agree; disagreement would point to flaws in the structure formation model assumed, or to systematic errors in the data.

Note that our constraints are a bit weaker than those obtained by JT03 and BJ03. One might think this could be due to the fact that we use the offset-linear scaling rather than the Jain-Taylor linear scaling – the former involves more parameters than the latter (compare eq. [6] and [9]). On the other hand, the offset-linear scaling allows the use of both shear-shear and galaxy-shear correlations while the Jain-Taylor linear scaling can be applied only to galaxy-shear. So, it is not *a priori* obvious how our constraints should compare with those of JT03 and BJ03. In Appendix A, we will discuss what happens if we carry out parameter estimation using the linear scaling. We find dark energy constraints that are weaker than those obtained by JT03 and BJ03 even in that case. The reasons are discussed in Appendix A.

4. GEOMETRY AS A CONSISTENCY CHECK

Our procedure, described in the last section, making use of the offset-linear scaling of eq. [6], is very conservative *i.e.* we marginalize over all possible 3-d mass, galaxy, and galaxy-mass power spectra in order to extract the pure geometrical information. In truth, we do know a fair amount about these power spectra, especially from non-lensing observations. The conventional approach is to assume the 3-d mass power spectrum is well constrained from other observations (such as the microwave background), and fit

for dark energy constraints from shear-shear correlations which depend on dark energy parameters through both geometrical distances and the growth rate of the mass power spectrum (which of course implicitly assumes a structure formation model such as Cold-Dark-Matter; see *e.g.* Hu 2002, Abazajian & Dodelson 2003). In other words, unlike the offset-linear scaling method which introduces a whole set of nuisance parameters in addition to dark energy parameters, the conventional approach has *only* the dark energy parameters as free parameters. A simple alternative, which is less conservative than the offset-linear scaling method, but allows a consistency test that the conventional approach does not offer, is as follows. Follow the conventional approach, but split the dark energy parameters into two kinds: those that enters the growth factor, and those that enters the geometrical distances, and fit for these separately. With such parameter-splitting (Stebbins 2003), one does not expect and will not obtain better constraints compared to the conventional approach where equivalence between these two sets of parameters is enforced. The rationale for parameter-splitting is to check for consistency: if we could verify that the values of w for example obtained separately from geometry and from growth (let us call them w(geometry) and w(growth)) are consistent with each other, this would increase our confidence in the values obtained; if they disagree, the discrepancy would help isolate what was going wrong, say systematic errors (*e.g.* Hoekstra 2003), or contamination of shear by intrinsic alignments (Lee & Pen 2000, Croft & Metzler, Heavens, Refregier, & Heymans 2000, Brown *et al.*, Catelan, Kamionkowski, & Blandford, Mackey, White & Kamionkowski 2001, Porciani, Dekel, & Hoffman 2002, Vitvitska *et al* 2002, Maller, Dekel, & Somerville 2002, van den Bosch *et al.* 2002, Hui & Zhang 2002), or incorrect assumptions about the mass power spectrum.

As an illustration, in Fig. 3, we show such a consistency test via parameter-splitting. We adopt the same fiducial model as in Fig. 1, and estimate the constraints on w(geometry) and w(growth) from both the shear-shear power spectrum $P_{\gamma\gamma}$ and the galaxy-shear power spectrum $P_{g\gamma}$. To fit the galaxy-shear data, we assume the galaxies are linearly biased with respect to the mass, and we marginalize over an independent galaxy-bias for each redshift bin ($n_{\rm bin} = 20$). We limit ourselves to information from $\ell < 200$, for two reasons: the galaxy-bias is probably not linear on smaller scales; the nonlinear mass power spectrum might not be accurately predicted even though we assume here the linear mass power spectrum is well constrained from other observations. Fig 3 shows that such a consistency test can yield constraints that are interesting precision-wise. It is also interesting how using both $P_{\gamma\gamma}$ and $P_{g\gamma}$ gives significantly better constraints than using just one of them.

5. DISCUSSION

In this paper, we have introduced a special scaling, which we call the offset-linear scaling: imagine one has a foreground population of galaxies from which one forms either a galaxy-density field or a shear field; when one cross-correlates this field with the shear measured from some background population, the cross-correlation signal ($P_{\rm g\gamma}$ or $P_{\gamma\gamma}$) scales with the redshift of the background population in a way that is specific to lensing. This is

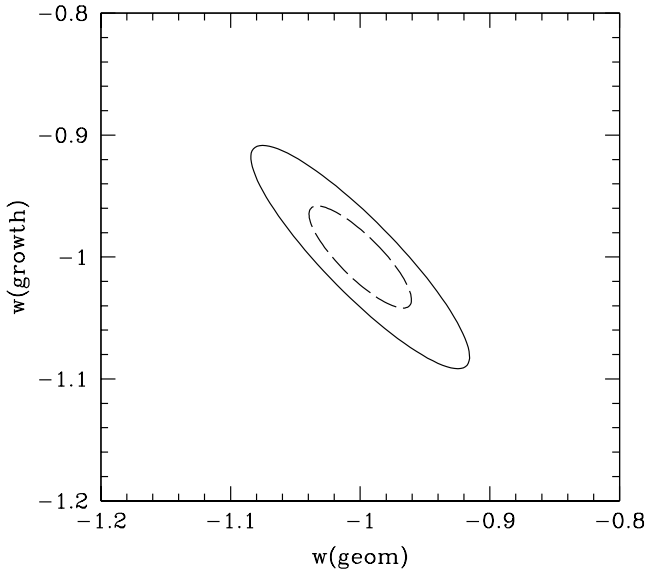

FIG. 3.— Constraints on the dark energy equation of state w following the conventional approach (*i.e.* not using offset-linear scaling; see text), but with the parameter split into two: one controlling the growth factor and the other controlling the geometrical distances. The solid (1σ) contour is from using just the shear-shear power spectrum $P_{\gamma\gamma}$. The dashed ($1\ \sigma$) contour is from using both shear-shear and galaxy-shear power spectra $P_{g\gamma}$. $\Omega_{\rm de}$ is fixed at 0.7. The survey size and depth are the same as those of Fig. 1.

the content of eq. [6]. Such a scaling can be exploited to extract purely geometrical information from a lensing survey. Effectively, one can measure angular diameter distances (or more accurately, combinations thereof; eq. [16]) from a lensing experiment without making any assumptions about the shape or growth of the mass/galaxy power spectrum. The idea is to measure the galaxy-shear and shear-shear power spectra, $P_{\rm g\gamma}$ and $P_{\gamma\gamma}$ for a variety of foreground and background redshift bins. Given a sufficient number of bins, one can fit for all the quantities A, B, F, G and $\chi_{\rm eff}$ in eq. [6]. One can then obtain dark energy constraints from $\chi_{\rm eff}$ alone, which is a purely geometrical quantity, essentially an angular diameter distance weighed in a particular way (eq. [7]).

Such an approach has certain virtues. The obvious one is that the resulting constraints are free of assumptions about one's structure formation model (typically a Cold Dark Matter model with a nearly scale invariant primordial power spectrum). Because of this, one can also make use of information on smaller scales than what one would otherwise feel uncomfortable using, either because of nonlinearity in the case of $P_{\gamma\gamma}$, or because of galaxy-biasing in the case of $P_{\rm g\gamma}$.

The level of constraints from this method employing the offset-linear scaling is shown in Fig. 1 and Fig. 2. The constraints are weaker than conventional methods such as lensing tomography (Hu 2002, Abazajian & Dodelson

2003). This is not surprising since the offset-linear scaling method isolates and uses only the geometrical information, whereas conventional methods make use of information from both growth and geometry and assumes the mass power spectrum is well constrained from other methods. Nonetheless, the constraints are sufficiently interesting to make our geometrical method a useful consistency check on assumptions behind conventional methods (*e.g.* Cold Dark Matter structure formation model). Comparing against JT03 and BJ03, who used a similar geometrical approach as here but a different scaling (we call the linear scaling; eq. [9]), it appears our constraints are weaker than theirs. We believe the reason is largely because the statistical errors have been underestimated by JT03 and BJ03. This is discussed in detail in Appendix A.

A useful feature of the offset-linear scaling is that it is not as demanding on the photometric redshift accuracy as the linear scaling (see §2.3, 2.5). Another useful feature: the offset-linear scaling can be applied to both shear-shear and galaxy-shear correlations, whereas the linear scaling can be applied only to the latter (see §2.2).

In §4, we introduce the idea of parameter splitting. In fitting for dark energy parameters to the observed lensing power spectra (as done in the conventional approach), one can artificially split them up into those that control the growth factor, and those that control the geometrical distances. Consistency between the two sets would be a good check for the presence of systematic errors, intrinsic alignment or incorrect assumptions about the nature of the mass fluctuations. This consistency test is less conservative than the one using the offset-linear scaling.

In a sense, the techniques outlined in §2 and §4 represent two extremes of a whole spectrum of ways to separate geometrical information from growth information: from making no assumptions about the mass (and galaxy-mass) power spectrum to assuming that it is known to high precision. There are likely techniques that are intermediate in this spectrum that might also prove useful.

We are grateful to Gary Bernstein, Bhuvnesh Jain, and especially Wayne Hu for useful discussions. Support for this work is provided in part by the DOE and its Outstanding Junior Investigator Program, by NASA grant NAG5-10842 and NSF grant AST-0098437. LH is grateful to the organizers of the superstring cosmology program at the KITP, where part of this work was done.

REFERENCES

Abazajian, K. & Dodelson, S. 2003, PRL, 91, 041301
Bacon, D.J., Refregier, A.R. & Ellis, R.S. 2000, MNRAS, 318, 625
Bartelmann, M. & Schneider, P. 2001, Phys. Rep., 340, 291
Bernstein, G., Jain, B. 2003, ApJ, in press, astro-ph 0309332 [BJ03]
Benabed, K. & Bernardeau, F. 2001, Phys. Rev. D64, 083501
Benabed, K. & van Waerbeke, L. 2003,
Blandford, R.D., Saust A.B., Brainerd, T.G. & Villumsen, J.V. 1991, MNRAS, 251, 600
Brainerd, T.G., Blandford, R.D. & Smail, I. 1996, ApJ, 466, 623
Brown, M.L., Taylor, A.N., Hambly, N.C., & Dye, S. 2000, submitted to MNRAS, astro-ph 0009499
Catelan, P., Kamionkowski, M. & Blandford, R.D. 2001, MNRAS, 320, 7
Crittenden, R.G., Natarajan, P., Pen, U, & Theuns, T. 2001, ApJ, 559, 552
Croft, R.A.C. & Metzler, C.A. 2000, ApJ, 545, 561
Cooray, A. & Hu, W. 2001, ApJ, 554, 56
Fischer, P. *et al.* 2000, AJ, 120, 1198
Guzik, J., Seljak, U. 2001, MNRAS, 321, 439
Heavens, A., Refregier, A., & Heymans, C. 2000, MNRAS, 319, 649
Hoekstra, H. 2003, submitted to MNRAS, astro-ph 0306097
Hoekstra, H., Yee, H., & Gladders, M. 2002, ApJ, 577, 595
Hu, W. 1999, ApJL, 522, 21
Hu, W. 2002, Phys. Rev. D66, 3515
Hu, W., Jain, B. 2003, preprint
Hui, L. 1999, ApJL, 519, 9
Hui, L, & Gaztanaga, E. 1999, ApJ, 519, 622
Hui, L. & Zhang, J. 2002, submitted to ApJ, astro-ph 0205512
Huterer, D. 2002, Phys. Rev. D65, 3001
Jain, B. & Seljak, U. 1997, ApJ, 484, 560
Jain, B. & Taylor, A. 2003, submitted to PRL, astro-ph 0306046 [JT03]
Jarvis, M., Bernstein, G.M., Fischer, P., Smith, D., Jain, B., Tyson, J.A., Wittman, D. 2003, AJ, 125, 1014
Kaiser, N. 1992, ApJ, 388, 272
Kaiser, N., Wilson, G. & Luppino, G. 2000, astro-ph 0003338
Kravtsov, A. V., Berlind, A. A., Wechsler, R. H., Klypin, A. A., Gottloeber, S., Allgood, B., Primack, J. R. 2003, submitted to ApJ, astro-ph 0308519
Lee, J., & Pen, U. 2000, ApJL, 532, 5
Linder, E. V. 2002, astro-ph 0210217
Ma, C.-P., Fry, J. N. 2000, ApJL, 531, 87
Mackey, J., White, M. & Kamionkowski, M. 2002, MNRAS, 332, 788
Maoli, R., van Waerbeke, L., Mellier, Y., Schneider, P., Jain, B., Bernardeau, F., Erhen, T. & Fort, B. 2001, A & A, 368, 766
Maller, A. H., Dekel, A. & Somerville, R. S. 2002, MNRAS, 329, 423
McKay, T. et al. 2001, submitted to ApJ, astro-ph 0108013
Miralda-Escude, J. 1991, ApJ, 380, 1
Munshi, D., Wang, Y. 2003, ApJ, 583, 566
Pen, U.-L., Lu, T., van Waerbeke, L., Mellier, Y. 2003, submitted to MNRAS, astro-ph 0304512
Porciani, C., Dekel, A. & Hoffman, Y. 2002, MNRAS, 332, 325
Refregier, A., Massey, R., Rhodes, J., Ellis, R., Albert, J., Bacon, D., Bernstein, G., McKay, T., Perlmutter, S. 2003, submitted to ApJ, astro-ph 0304419
Rhodes, J., Refregier, A. & Groth, E. J. 2001, ApJL, 552, 85
Soccimarro, R., Sheth, R., Hui, L., Jain, B. 2001, ApJ, 546, 20
Scoccimarro, R., Zaldarriaga, M., Hui, L. 1999, ApJ, 527, 1
Seljak, U. 2000, MNRAS, 318, 203
Sheldon, E., Johnston, D. E., Frieman, J. A., Scranton, R., McKay, T. A., Connolly, A. J., Budavari, T., Zehavi, I., Bahcall, N., Brinkmann, J., Fukugita, M. 2003, submitted to AJ, astro-ph 0312036
Sheth, R. K., Jain, B. 1997, MNRAS, 285, 231
Song, Y.-S., Knox, L. 2003, submitted to PRD, astro-ph 0312175
Stebbins, A. 1996, astro-ph/9609149
Stebbins, A. 2003, in preparation
Szapudi, I., Szalay, A. 1998, ApJL, 494, 41
Takada, M., Jain, B. 2003, submitted to MNRAS, astro-ph 0310125
Takada, M., White, M. 2003, submitted to ApJL, astro-ph 0311104
Tegmark, M. 1997, Phys. Rev. D55, 5895
van den Bosch, F.C., Abel, T., Croft, R.A.C., Hernquist, L. & White, S.D.M. 2002, ApJ, 576, 21
van Waerbeke, L., Mellier, Y., Erben, T. et al. 2000, A& A, 358, 30
van Waerbeke, L., Takashi, H., Scoccimarro, R., Colombi, S., Bernardeau, F. 2001, MNRAS, 322, 918
Vitvitska, M. et al. 2002, ApJ, 581, 799
White, M. & Hu, W. 2000, ApJ, 537, 1
Wittman, D.M., Tyson, J.A., Kirkman, D., Dell'Antonio, I. & Bernstein, G. 2000, Nature, 405, 143

APPENDIX A – COMPARISON WITH JT03

Our aim in this Appendix is to discuss our differences from Jain & Taylor (2003) [JT03] and to a lesser extent Bernstein & Jain (2003) [BJ03].

We all share the common goal of isolating geometrical constraints on dark energy from lensing data. JT03/BJ03 focused on the use of the linear scaling (eq. [9]) while we focus on the offset-linear scaling (eq. [6]). The linear scaling introduces fewer nuisance parameters but can only be applied to galaxy-shear, not shear-shear, correlation data. It is therefore not *a priori* obvious whose constraints should be stronger. The most direct comparison can be made between the solid contour of our Fig. 1 and the smallest

contour in Fig. 1 of JT03[7]. Our constraints appear to be weaker by about a factor of 3 compared to JT03. What is puzzling is that even when we adopt exactly the JT03 linear scaling, and redo our calculation, the constraints are still weaker than those of JT03 by a factor of at least 3 or more. (The discrepancy depends on exactly how the JT03 scaling is implemented, particularly on the choice of redshift bins; the choice of bins in JT03 seems to lead to statistical errors larger than factor of 3, see below). This translates into at least an order of magnitude difference in the variance. This is not a small discrepancy, particularly when we use exactly the JT03 method. In this Appendix, we will focus on this discrepancy with JT03, but will also briefly comment on the treatment of BJ03 (who obtained similar constraints as JT03).

We believe the statistical error quoted in JT03 have been underestimated. There appears to be several different reasons, the first two of which were pointed out to us by Wayne Hu (see Hu & Jain 2003). First, JT03 adopted a singular isothermal spherical profile for cluster halos that they considered. More realistic profiles such as NFW produce a smaller lensing signal. Second, it appears profile aside, the lensing signal itself is overestimated. Third, which is the aspect we would like to focus on, we believe not all sources of statistical errors were taken into account by JT03. Hu & Jain (2003) also independently reached the same conclusions.

To recapitulate, JT03 proposed to examine the ratio of the galaxy-shear correlation at two different redshifts. For simplicity, we will consider the ratio of the galaxy-convergence correlation instead, which can of course be obtained from the galaxy-tangential-shear correlation: [8]

$$R^i = P^{i,1}_{\mathrm{g}\kappa}/P^{i,2}_{\mathrm{g}\kappa} \tag{27}$$

where i specifies some foreground population, and 1 and 2 refers to convergence from 2 different background redshift bins. We use the symbol $P_{\mathrm{g}\kappa}$ loosely to refer to either galaxy-convergence correlation function, or the galaxy-convergence power spectrum. Which is which should be clear from the context (actual power spectrum will usually have argument ℓ). [9]

The statistical error on dark energy parameters clearly comes from the statistical error on R^i, which in turn is determined by the statistical error of the $P_{\mathrm{g}\kappa}$ correlations. Before launching onto a detailed calculation, it is helpful to indicate roughly where we disagree with JT03 (and also BJ03). Think of $P_{\mathrm{g}\kappa}$ as $\sim \langle\delta_g\kappa\rangle$. Its variance under Gaussian random approximation (relaxing the Gaussian assumption would only increase the error) should be $\langle\delta_g\kappa\delta_g\kappa\rangle - \langle\delta_g\kappa\rangle\langle\delta_g\kappa\rangle \sim \langle\kappa\kappa\rangle\langle\delta_g\delta_g\rangle + \langle\delta_g\kappa\rangle\langle\delta_g\kappa\rangle$. As we will argue, what JT03 appeared to have considered is only the part of the variance that comes from the product of shape-noise in $\langle\kappa\kappa\rangle$, and shot-noise in $\langle\delta_g\delta_g\rangle$ *i.e.* $\sigma^2_\kappa/(\bar{n}^B\bar{n}^g)$, where σ^2_κ is the shape-noise of each background galaxy, $\bar{n}^B$ is the number density of background and $\bar{n}^g$ is the number density of foreground galaxies. In other words, JT03 appeared to have ignored sampling variance terms. Not only do these terms ignored by JT03 increase the variance of the measured $P_{\mathrm{g}\kappa}$ (and R^i), they also introduce correlation in errors between R^i's measured from different foreground bins, which was also absent in JT03.

Let us now derive the errorbar on R^i in detail. The estimator for $P_{\mathrm{g}\kappa}$ can be written as

$$\hat{P}_{\mathrm{g}\kappa} = \sum_{\alpha\beta} \delta^g_\alpha \kappa_\beta \tilde{W}_{\alpha\beta} \tag{28}$$

The picture in mind is to think of the survey being divided into pixels, and δ^g_α is the galaxy overdensity in pixel α, while κ_β is the convergence in pixel β. The symbol $\tilde{W}_{\alpha\beta}$ can stand for many different things. For example, if one is interested in the real space correlation function at separation $\Delta\theta$, $\tilde{W}_{\alpha\beta}$ should be equal to zero when the separation between α and β differs from $\Delta\theta$, or else equal to $1/N$, where N is the total number of pairs of pixels at that separation. If one is interested in the power spectrum at wavenumber ℓ, $\tilde{W}_{\alpha\beta} = (1/N^2_{\mathrm{pix}})\exp(-i\ell\cdot\Delta\theta_{\alpha\beta})$ where N_{pix} is the total number of pixels, and A_T is the total survey area. [10] JT03 considered a particular $\tilde{W}_{\alpha\beta}$ that corresponds to averaging the galaxy-convergence correlation over some aperture. We will keep $\tilde{W}_{\alpha\beta}$ general for now.

One word about the estimator $\hat{P}_{g\kappa}$. It might appear very different from the way one usually thinks of galaxy-galaxy lensing. The usual approach is to sit on a foreground galaxy, measure the background tangential shear averaged around a circle, then average over all foreground galaxies (Brainerd, Blandford & Smail 1996, Fischer et al. 2000, McKay et al. 2001). This is equivalent to measuring $\sum_{\alpha\beta}(n^g_\alpha/\bar{n}^g)\gamma^t_\beta\tilde{W}_{\alpha\beta}$ where γ^t is the background tangential shear, and n^g_α is equal to unity if pixel α has a foreground galaxy or vanishes otherwise, and $\bar{n}^g$ is its average over the survey. It is easy to see that such an estimator on average is equivalent to $\sum_{\alpha\beta}\delta^g_\alpha\gamma^t_\beta\tilde{W}_{\alpha\beta}$, where $\delta^g_\alpha = n^g_\alpha/\bar{n}^g - 1$. The only difference between this and the estimator in eq. [28] is the replacement of γ^t by κ. This is merely for the sake of simplifying our following expressions. Finally, note that using δ^g in place of $n^g/\bar{n}^g$ is generally a good idea because it reduces the variance of the estimator (Szapudi & Szalay 1998).

The estimator for R^i is given by

$$\hat{R}^i = \hat{P}^{i,1}_{\mathrm{g}\kappa}/\hat{P}^{i,2}_{\mathrm{g}\kappa} \tag{29}$$

We caution here that the above estimator is unbiased only to the lowest order in fluctuations, but we will ignore such complications here (*e.g.* Hui & Gaztanaga 1999).

[7] The method of JT03 requires high photometric redshift accuracy, hence the $\sigma_z = 0.01$ contour of our Fig. 1 is the relevant one to compare against.

[8] In previous sections of the paper, we have been loosely using the term shear γ as equivalent to convergence. In the appendix here, to avoid confusion especially in Appendix B, we explicitly use the symbol κ when we are discussing convergence.

[9] JT03 actually considered halo-shear rather than galaxy-shear. We will continue to use the term galaxy-shear. All our expressions are equally valid for special classes of foreground 'galaxies' such as groups or clusters.

[10] Strictly speaking, one is usually interested in the power spectrum at a given $|\ell|$, and so $\tilde{W}_{\alpha\beta}$ should involve an average over directions of ℓ. Note also that the $\tilde{W}_{\alpha\beta}$ differs from the conventional one by a factor of A_T, but that is fine since we are only interested in fractional error. Our choice is to enforce $\sum_{\alpha\beta}\tilde{W}_{\alpha\beta} = 1$, which simplifies some of our expressions below.

Eq.s [28,29] imply the following expression for the fractional variance of the ratio R^i:

$$V(i) \equiv \langle(\delta\hat{R}^i)^2\rangle/(R^i)^2 = V^1(i) + V^2(i) - 2V^{1,2}(i) \quad (30)$$

where V^1 is the fractional variance of $\hat{P}^{i,1}_{g\kappa}$, V^2 is the corresponding quantity for $\hat{P}^{i,2}_{g\kappa}$, and $V^{1,2}$ is the cross-variance between them, and they are given by (approximating fluctuations as Gaussian random):

$$V^1(i) = [\int \frac{d^2\ell}{(2\pi)^2} P^{i,1}_{g\kappa}(\ell) J(\ell)]^{-2} \times \quad (31)$$
$$\int \frac{d^2\ell}{(2\pi)^2} \frac{|J_\ell|^2}{A_T} [P^{i,1}_{g\kappa}(\ell)^2 + (P^{i,i}_{gg}(\ell) + \frac{1}{\bar{n}^g_i})(P^{1,1}_{\kappa\kappa}(\ell) + \frac{\sigma^2_\kappa}{\bar{n}^B_1})]$$
$$V^2(i) = [\int \frac{d^2\ell}{(2\pi)^2} P^{i,2}_{g\kappa}(\ell) J(\ell)]^{-2} \times$$
$$\int \frac{d^2\ell}{(2\pi)^2} \frac{|J_\ell|^2}{A_T} [P^{i,2}_{g\kappa}(\ell)^2 + (P^{i,i}_{gg}(\ell) + \frac{1}{\bar{n}^g_i})(P^{2,2}_{\kappa\kappa}(\ell) + \frac{\sigma^2_\kappa}{\bar{n}^B_2})]$$
$$V^{1,2}(i) = [\int \frac{d^2\ell}{(2\pi)^2} P^{i,1}_{g\kappa}(\ell) J(\ell)]^{-1} \times$$
$$[\int \frac{d^2\ell}{(2\pi)^2} P^{i,2}_{g\kappa}(\ell) J(\ell)]^{-1} \times$$
$$\int \frac{d^2\ell}{(2\pi)^2} \frac{|J_\ell|^2}{A_T} [P^{i,1}_{g\kappa}(\ell) P^{i,2}_{g\kappa}(\ell) + (P^{i,i}_{gg}(\ell) + \frac{1}{\bar{n}^g_i}) P^{1,2}_{\kappa\kappa}(\ell)]$$

Here, $P^{i,1}_{g\kappa}$ is the power spectrum between galaxies in foreground bin i and convergence in the background bin 1 (there are only 2 background bins in JT03), $P^{i,i}_{gg}$ is the power spectrum of foreground galaxies with themselves in bin i, and so on. The symbol σ^2_κ represents the variance in convergence due to the intrinsic noise of each galaxy, and $\bar{n}^g_i$ is the galaxy density in foreground bin i, $\bar{n}^B_1$ is the density of galaxies in background bin 1, and so on. The total survey area is A_T. The quantity $J(\ell)$ is the Fourier transform of the estimator kernel $\tilde{W}_{\alpha\beta}$:

$$J(\ell) \equiv \left[\sum_{\Delta\theta_{\alpha\beta}} \tilde{W}_{\alpha\beta}\right]^{-1} \sum_{\Delta\theta_{\alpha\beta}} \tilde{W}_{\alpha\beta} \exp[-i\ell\cdot\Delta\theta_{\alpha\beta}] \quad (32)$$

Among all the terms for $V(i)$, which correspond to those considered by JT03? They are the sum of terms in $V^1(i)$ and $V^2(i)$ that consist of the product of shape-noise and shot-noise (we will refer to these loosely as shot-noise terms):

$$V^{\rm JT03}(i) \equiv \quad (33)$$
$$[\int \frac{d^2\ell}{(2\pi)^2} P^{i,1}_{g\kappa}(\ell) J(\ell)]^{-2} \frac{\sigma^2_\kappa}{A_T \bar{n}^g_i \bar{n}^B_1} \int \frac{d^2\ell}{(2\pi)^2} |J(\ell)|^2$$
$$+[\int \frac{d^2\ell}{(2\pi)^2} P^{i,2}_{g\kappa}(\ell) J(\ell)]^{-2} \frac{\sigma^2_\kappa}{\bar{A}_T \bar{n}^g_i \bar{n}^B_2} \int \frac{d^2\ell}{(2\pi)^2} |J(\ell)|^2$$

To see that this does correspond to what JT03 considered, note that JT03 focused on the measurement of the real-space galaxy-convergence correlation smoothed within some aperture (of, say, area A_p). This corresponds to a choice of $J(\ell)$ (or $\tilde{W}_{\alpha\beta}$ in eq. [28]) such that $(2\pi)^{-2}\int d^2\ell |J(\ell)|^2 \sim 1/A_p$. Therefore, the above expression reduces to

$$V^{\rm JT03}(i) = \frac{\sigma^2_\kappa}{A_T A_P \bar{n}^g_i \bar{n}^B_1 [P^{i,1}_{g\kappa}(A_P)]^2} \quad (34)$$
$$+ \frac{\sigma^2_\kappa}{\bar{A}_T A_P \bar{n}^g_i \bar{n}^B_2 [P^{i,2}_{g\kappa}(A_P)]^2}$$

where we have abused the notation a little bit to denote the real-space galaxy-convergence correlation smoothed in an aperture of area A_P by $P^{i,1}_{g\kappa}(A_P)$. The above can be compared directly with equation 12 of JT03. The dictionary for translating our symbols to theirs is as follows: $\sigma^2_\kappa \to \sigma^2_\epsilon/2$, $\bar{n}^B_1 \to n_1$, $\bar{n}^B_2 \to n_2$, $[P^{i,1}_{g\kappa}(A_P)]^2 \to \langle\gamma\rangle^2_{\ell 1}$, $[P^{i,2}_{g\kappa}(A_P)]^2 \to \langle\gamma\rangle^2_{\ell 2}$, $A_T \to A$, and $A_P \bar{n}^g_i \to f_\ell$. The last item requires a little explanation. JT03 defined f_ℓ to be the fraction of the survey that is covered by the apertures centered on foreground objects. This is equal to $A_P \times (\bar{n}^g_i A_T)/A_T$, where A_T is the total survey area. With this, the correspondence with the expression of JT03 is manifest.

The expressions for statistical errors are actually simpler in Fourier space *i.e.* suppose instead of measuring the galaxy- convergence correlation smoothed in some aperture, one measures the galaxy-convergence power spectrum at wavenumber ℓ. One can obtain the ratio R^i for each ℓ, and then combine all these estimates of R^i from each ℓ in a minimum variance manner. Note that while this is different from the procedure of JT03, the procedure here will likely produce smaller errorbars on R^i, since it makes use of all information contained in the modes instead of focusing on fluctuations at particular scales.

Let us focus on a particular wavenumber (or band) ℓ for the moment. Eq.s [30,31] reduce to something quite simple:

$$V_\ell(i) = [P^{i,1}_{g\kappa}(\ell)]^{-2}(P^{i,i}_{gg}(\ell) + \frac{1}{\bar{n}^g_i})(P^{1,1}_{\kappa\kappa}(\ell) + \frac{\sigma^2_\kappa}{\bar{n}^B_1}) \quad (35)$$
$$+[P^{i,2}_{g\kappa}(\ell)]^{-2}(P^{i,i}_{gg}(\ell) + \frac{1}{\bar{n}^g_i})(P^{2,2}_{\kappa\kappa}(\ell) + \frac{\sigma^2_\kappa}{\bar{n}^B_2})$$
$$-2[P^{i,1}_{g\kappa}(\ell)]^{-1}[P^{i,2}_{g\kappa}(\ell)]^{-1}(P^{i,i}_{gg}(\ell) + \frac{1}{\bar{n}^g_i})P^{1,2}_{\kappa\kappa}(\ell)$$

where we have used $J(\ell) = |J(\ell)|^2 = (2\pi)^2\delta^2(\ell - \ell')/A_T$, and we have introduced subscript ℓ to V to emphasize this is the variance of R^i from Fourier bin ℓ.

The Fourier analog of the approximation made by JT03 would be to retain only the following terms in the variance:

$$V^{\rm JT03}_\ell(i) = [P^{i,1}_{g\kappa}(\ell)]^{-2} \frac{1}{\bar{n}^g_i} \frac{\sigma^2_\kappa}{\bar{n}^B_1} + [P^{i,2}_{g\kappa}(\ell)]^{-2} \frac{1}{\bar{n}^g_i} \frac{\sigma^2_\kappa}{\bar{n}^B_2} \quad (36)$$

This misses a number of terms compared to $V_\ell(i)$ in eq. [35]. Each of the terms ignored by JT03 are of order unity. They can be thought of as sampling variance terms. While there is some partial cancellation among them, they do not cancel exactly and should be retained.

JT03 considered the constraint on dark energy from the ratio R^i for i ranging over 10 different foreground redshift bins, ranging from $z = 0$ to $z = 1$, each with $\Delta z = 0.1$. In addition to the diagonal variance considered above, there

will in general be covariance between R measured from foreground bin i and foreground bin j, which was not considered by JT03:

$$\begin{aligned} V_\ell(i,j) &\equiv \langle \delta\hat{R}^i \delta\hat{R}^j\rangle/(R^i R^j) \qquad (37)\\ &= \delta_{ij} V_\ell(i) + [P^{i,i1}_{g\kappa}(\ell)]^{-1}[P^{j,j1}_{g\kappa}(\ell)]^{-1} P^{i,j1}_{g\kappa} P^{j,i1}_{g\kappa} \\ &+[P^{i,i2}_{g\kappa}(\ell)]^{-1}[P^{j,j2}_{g\kappa}(\ell)]^{-1} P^{i,j2}_{g\kappa} P^{j,i2}_{g\kappa} \\ &-[P^{i,i1}_{g\kappa}(\ell)]^{-1}[P^{j,j2}_{g\kappa}(\ell)]^{-1} P^{i,j2}_{g\kappa} P^{j,i1}_{g\kappa} \\ &-[P^{i,i2}_{g\kappa}(\ell)]^{-1}[P^{j,j1}_{g\kappa}(\ell)]^{-1} P^{i,j1}_{g\kappa} P^{j,i2}_{g\kappa} \end{aligned}$$

Note the somewhat clumsy notation: instead of specifying the 2 background bins by just 1 and 2, we now have to specify them by $i1$ and $i2$ which refers to the 2 background bins that correspond to the i-th foreground bin, and similarly for $j1$ and $j2$. The covariance $V_\ell(i,j)$, when $i \neq j$, is non-vanishing – the positive and negative terms present do not exactly cancel each other, and generically result in something of same order of each of these terms, with perhaps some mild suppression.

Making use of $V_\ell(i,j)$ one can then work out the dark energy constraints from the linear scaling of JT03. Adopting the survey specifications and redshift-binning according to JT03, we find constraints that are shown in Fig. 4. This can be compared against the smallest contour in Fig. 1 of JT03. Hu & Jain (2003) independently reached similar conclusions as in Fig. 4.

In summary, it appears JT03 ignored certain contributions to the variance (and covariance) of the ratio R^i. They are primarily sampling variance terms. These are automatically taken into account in our Fisher matrix analysis in §3, which actually does not require an explicit computation of all these variance terms. This should be contrasted with the Fisher matrix calculation of BJ03: while we start with the galaxy-density and shear fields as input Gaussian random data and compute constraints on parameters which enter into the correlation matrix (eq. [22]), BJ03 started with the quadratic estimates of lensing power spectra themselves as Gaussian distributed input data. The latter approach requires explicit computation of the variance and covariance of these quadratic estimates, and care should be taken to include all contributions. It appears some of these contributions were not included in the analysis of BJ03. We have not, however, performed an analysis replicating the details of BJ03.

APPENDIX B – NON-FLAT UNIVERSE, SHEAR AND REAL SPACE CORRELATIONS

Our goal in this Appendix is to state our main results in this paper for the more general case of a non-flat universe, for shear instead of convergence, and in real as well as Fourier space. Some of the expressions have appeared in the literature. They are given here for completeness.

Let us start with what is most commonly measured in galaxy-galaxy lensing experiments, and relate it to the galaxy-convergence power spectrum $P_{g\kappa}(\ell)$ given in eq. [2] (Kaiser 1992):

$$\xi_{g\gamma^+}(\theta) = -\int \frac{\ell d\ell}{2\pi} P_{g\kappa}(\ell) J_2(\ell\theta) \qquad (38)$$

where J_2 is the second order Bessel function, [11] and

[11] $J_n(y) = \frac{1}{2\pi}\int_{-\pi}^{\pi} d\eta \cos[y\sin\eta - n\eta]$

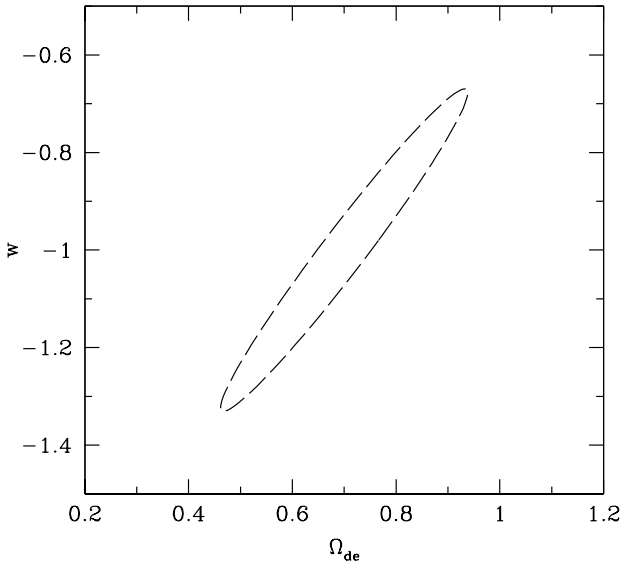

FIG. 4.— Dark energy constraints (1 σ) by adopting the linear scaling, survey specifications and redshift binning of JT03. No prior is placed on Ω_{de} or w. The fiducial model has $w = -1$ and $\Omega_{de} = 0.7$; w' is fixed at 0.

$\xi_{g\gamma^+}(\theta)$ is the cross-correlation between galaxies and tangential shear at separation θ, a quantity that is most commonly discussed in galaxy-galaxy lensing measurements. Alternatively, in a fixed coordinate system where γ^1 and γ^2 are the two components of shear, the 2 different galaxy-shear power spectra $P_{g\gamma^1}(\ell)$ and $P_{g\gamma^2}(\ell)$ are related to the galaxy-convergence power spectrum $P_{g\kappa}$ by:

$$P_{g\gamma^1}(\ell) = \cos(2\phi_\ell) P_{g\kappa}(\ell)\,,\; P_{g\gamma^2}(\ell) = \sin(2\phi_\ell) P_{g\kappa}(\ell) \quad (39)$$

where ϕ_ℓ specifies the orientation of the wavevector: $\ell\cos\phi_\ell$ is the x-component while $\ell\sin\phi_\ell$ is the y-component.

Similarly, the two quantities that are commonly considered in actual shear-shear correlation measurements are related to the convergence power spectrum $P_{\kappa\kappa}(\ell)$ of eq. [3] by (Kaiser 1992):

$$\begin{aligned} \xi_{\gamma^+\gamma^+}(\theta) &= \frac{1}{2}\int \frac{\ell d\ell}{2\pi} P_{\kappa\kappa}(\ell)[J_0(\ell\theta) + J_4(\ell\theta)] \qquad (40)\\ \xi_{\gamma^\times\gamma^\times}(\theta) &= \frac{1}{2}\int \frac{\ell d\ell}{2\pi} P_{\kappa\kappa}(\ell)[J_0(\ell\theta) - J_4(\ell\theta)] \end{aligned}$$

where γ^+ and $\gamma^\times$ are the tangential and ortho-tangential (or radial) shear defined with respect to separation between two points of interest. Alternatively, the two different shear-shear power spectra in a fixed coordinate system are related to the convergence power spectrum by

$$\begin{aligned} P_{\gamma^1\gamma^1}(\ell) &= \cos^2(2\phi_\ell) P_{\kappa\kappa}(\ell) \qquad (41)\\ P_{\gamma^2\gamma^2}(\ell) &= \sin^2(2\phi_\ell) P_{\kappa\kappa}(\ell) \end{aligned}$$

The main results of this paper derive from writing $P_{g\kappa}(\ell; f, b)$ and $P_{\kappa\kappa}(\ell; f, b)$, which are the galaxy-convergence

and convergence-convergence power spectra between a foreground bin f and background bin b, in the form of eq. [17], and noticing some of the terms are small, which leads to the offset-linear scaling of eq. [6].

Let us first give the expressions for each term in eq. [17] (and eq. [6]) in the case of a non-flat universe. Then, we will discuss how similar expressions hold for shear measurements, and in real space.

The non-flat space analogs of eq.s [7,8] are

$$F(\ell;f) \equiv \frac{3\Omega_{\rm m0}H_0^2}{2c^2}\int \frac{d\chi}{a}W_f(\chi)\frac{1}{r(\chi)} \tag{42}$$
$$\mathrm{cs}(\chi)P_{g\delta}(\frac{\ell}{r(\chi)})$$
$$G(\ell;f) \equiv -\frac{3\Omega_{\rm m0}H_0^2}{2c^2}\int \frac{d\chi}{a}W_f(\chi)\frac{1}{r(\chi)}$$
$$\mathrm{si}(\chi)P_{g\delta}(\frac{\ell}{r(\chi)})$$
$$I(\ell;f,b) \equiv -\frac{3\Omega_{\rm m0}H_0^2}{2c^2}\int \frac{d\chi}{a}W_f(\chi)\int d\chi' W_b(\chi')$$
$$\frac{r(\chi'-\chi)}{r(\chi')r(\chi)}P_{g\delta}(\frac{\ell}{r(\chi)})\Theta(\chi-\chi')$$

$$\frac{1}{\chi_{\rm eff}(b)} \equiv \int d\chi' W_b(\chi')\frac{1}{\mathrm{ta}(\chi')} \tag{43}$$

$$A(\ell;f) \equiv \left(\frac{3\Omega_{\rm m0}H_0^2}{2c^2}\right)^2\int d\chi'' W_f(\chi'') \tag{44}$$
$$\int \frac{d\chi}{a^2}\frac{r(\chi''-\chi)}{r(\chi'')}\mathrm{cs}(\chi)P_{\delta\delta}(\frac{\ell}{r(\chi)})\Theta(\chi''-\chi)$$
$$B(\ell;f) \equiv -\left(\frac{3\Omega_{\rm m0}H_0^2}{2c^2}\right)^2\int d\chi'' W_f(\chi'')$$
$$\int \frac{d\chi}{a^2}\frac{r(\chi''-\chi)}{r(\chi'')}\,\mathrm{si}(\chi)P_{\delta\delta}(\frac{\ell}{r(\chi)})\,\Theta(\chi''-\chi)$$
$$D(\ell;f,b) \equiv -\left(\frac{3\Omega_{\rm m0}H_0^2}{2c^2}\right)^2\int d\chi'' W_f(\chi'')\int d\chi' W_b(\chi')$$
$$\int \frac{d\chi}{a^2}\frac{r(\chi'-\chi)}{r(\chi')}\frac{r(\chi''-\chi)}{r(\chi'')}P_{\delta\delta}(\frac{\ell}{r(\chi)})$$
$$\Theta(\chi-\chi')\,\Theta(\chi''-\chi)$$

where $r(\chi)$ is the comoving angular diameter distance which is related to the comoving radial distance χ as follows: $r(\chi) = K^{-1/2}\sin K^{1/2}\chi, (-K)^{-1/2}\sinh(-K)^{1/2}\chi, \chi$ for a closed, open and flat universe respectively, and $K = -\Omega_k H_0^2/c^2$, where Ω_k is the curvature in unit of the critical density. The quantities, $\mathrm{cs}(\chi)$, $\mathrm{si}(\chi)$, and $\mathrm{ta}(\chi)$ are defined as:

$$\mathrm{cs}(\chi) = \cos K^{\frac{1}{2}}\chi,\ \mathrm{si}(\chi) = \sin K^{\frac{1}{2}}\chi,\ \mathrm{ta}(\chi) = \tan K^{\frac{1}{2}}\chi \tag{45}$$

if $K > 0$,

$$\mathrm{cs}(\chi) = 1,\ \mathrm{si}(\chi) = \chi,\ \mathrm{ta}(\chi) = \chi \tag{46}$$

if $K = 0$, and

$$\mathrm{cs}(\chi) = \cosh(-K)^{\frac{1}{2}}\chi,\ \mathrm{si}(\chi) = \sinh(-K)^{\frac{1}{2}}\chi, \tag{47}$$
$$\mathrm{ta}(\chi) = \tanh(-K)^{\frac{1}{2}}\chi$$

if $K < 0$.

As before, the offset-linear scaling (eq. [6]) follows from eq. [17] by noticing that D and I are small provided that W_i and W_j have little overlap, except that the relevant quantities A, B, D, F, G and I are defined as above. With the above expressions, one can in principle fit for Ω_k in addition to the dark energy parameters in carrying out the exercise of §3.

Lastly, it is trivial to generalize the offset-linear scaling of eq. [6] to galaxy-shear and shear-shear (instead of galaxy-convergence and convergence-convergence as before) power spectra by using eq.s [39,41] *i.e.* simply multiply eq. [6] by appropriate factors of $\sin(2\phi_\ell)$ or $\cos(2\phi_\ell)$. Rewriting the scaling in real-space is no less difficult: simply substitute eq. [6] into the expressions for $\xi_{g\gamma^+}(\theta)$, $\xi_{\gamma^+\gamma^+}$ or $\xi_{\gamma^\times\gamma^\times}$ in eq. [38] and (40). One can see that the scaling continues to hold for real-space analogs of A, B, etc. In particular, eq. [16] holds for any of these real space correlation functions *e.g.*

$$\frac{\xi_{g\gamma^+}(\theta;f,b)-\xi_{g\gamma^+}(\theta;f,b')}{\xi_{g\gamma^+}(\theta;f,b'')-\xi_{g\gamma^+}(\theta;f,b''')} = \frac{\chi_{\rm eff}(b)^{-1}-\chi_{\rm eff}(b')^{-1}}{\chi_{\rm eff}(b'')^{-1}-\chi_{\rm eff}(b''')^{-1}} \tag{48}$$

where $\xi_{g\gamma^+}(\theta;f,b)$ refers to the galaxy-tangential-shear correlation between foreground redshift bin f and background redshift bin b.